Journal of Medicinal Chemistry

ARTICLE

pubs.acs.org/jmc

Structure-Based Design of a New Series of D-Glutamic Acid Based Inhibitors of Bacterial UDP-*N*-acetylmuramoyl-L-alanine:D-glutamate Ligase (MurD)†

Tihomir Tomašić,[‡] Nace Zidar,[‡] Roman Šink,[‡] Andreja Kovač,[‡] Didier Blanot,[§] Carlos Contreras-Martel,[∥,⊥,#] Andréa Dessen,[∥,⊥,#] Manica Müller-Premru,[∞] Anamarija Zega,[‡] Stanislav Gobec,[‡] Danijel Kikelj,[‡] and Lucija Peterlin Mašič*[,‡]

[‡]Faculty of Pharmacy, University of Ljubljana, 1000 Ljubljana, Slovenia

[§]Enveloppes Bactériennes et Antibiotiques, IBBMC, UMR 8619 CNRS, Université Paris-Sud, 91405 Orsay, France

[∥]Bacterial Pathogenesis Group, [⊥]Commissariat a l'Energie Atomique (CEA), and [#]Centre National pour la Recherche Scientifique (CNRS), Institut de Biologie Structurale, Université Grenoble I, Rue Jules Horowitz, 38027 Grenoble, France

[∞]Medical Faculty, Institute of Microbiology and Immunology, University of Ljubljana, 1105 Ljubljana, Slovenia

Supporting Information

ABSTRACT:

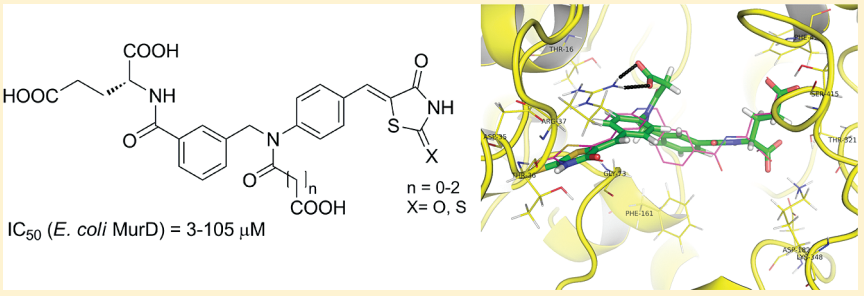

MurD ligase is one of the key enzymes participating in the intracellular steps of peptidoglycan biosynthesis and constitutes a viable target in the search for novel antibacterial drugs to combat bacterial drug-resistance. We have designed, synthesized, and evaluated a new series of D-glutamic acid-based *Escherichia coli* MurD inhibitors incorporating the 5-benzylidenethiazolidin-4-one scaffold. The crystal structure of **16** in the MurD active site has provided a good starting point for the design of structurally optimized inhibitors **73**−**75** endowed with improved MurD inhibitory potency (IC_{50} between 3 and 7 μM). Inhibitors **74** and **75** showed weak activity against Gram-positive *Staphylococcus aureus* and *Enterococcus faecalis*. Compounds **73**−**75**, with IC_{50} values in the low micromolar range, represent the most potent D-Glu-based MurD inhibitors reported to date.

1. INTRODUCTION

The escalating emergence of bacterial strains resistant to most of the currently available antibiotics has compromised the treatment of bacterial infections and led to increased morbidity and mortality worldwide.[1] Development of effective antibacterial drugs, necessitating novel mechanisms of action and more chemical diversity than current drugs, is therefore essential to combat bacterial drug-resistance.[2−4] Peptidoglycan is an essential cell wall polymer unique to prokaryotic cells that preserves cell integrity by withstanding high internal osmotic pressure and maintaining a defined cell shape.[5] The biosynthesis of peptidoglycan (a viable source of targets for development of novel antibacterials) is a multistep process comprising intracellular assembly of the UDP-MurNAc-pentapeptide, which is subsequently translocated through the cytoplasmic membrane and incorporated into the growing peptidoglycan layer. ATP-dependent Mur ligases (MurC to MurF) catalyze a series of reactions leading to UDP-MurNAc-pentapeptide by sequentially adding L-Ala (MurC), D-Glu (MurD), L-Lys or *meso*-diaminopimelic acid (MurE), and D-Ala-D-Ala dipeptide (MurF) to the starting MurC substrate UDP-MurNAc.[6,7] The fact that Mur ligases are vital for the survival of bacteria makes them attractive targets for antibacterial drug discovery.[7,8]

MurD ligase, like other Mur ligases, catalyzes the formation of a peptide bond between the carboxyl group of the UDP substrate and the amino group of the condensing D-glutamic acid. Mur ligases operate through a similar chemical mechanism[9,10] and, as shown for MurC and MurF, an ordered kinetic mechanism.[11,12] In the initial step, ATP is bound to the free enzyme, followed by

Received: March 3, 2011
Published: May 18, 2011

dx.doi.org/10.1021/jm2002525 | *J. Med. Chem.* 2011, 54, 4600–4610

the corresponding UDP substrate. The terminal carboxyl group of the UDP substrate is then activated by ATP-promoted phosphorylation, generating an acyl phosphate intermediate that is attacked by the amino group of the incoming amino acid or dipeptide. The resulting tetrahedral, high-energy intermediate breaks down with elimination of inorganic phosphate and concomitant formation of a peptide or amide bond. The crystal structures show MurD ligase to have a three-domain topology, with the N-terminal and central domains binding the UDP precursor and ATP, respectively, while the C-terminal domain binds the condensing amino acid or dipeptide.[9,13−16]

Since MurD catalyzes the formation of UDP-MurNAc-L-Ala-D-Glu (UMAG) by addition of D-Glu to the substrate UDP-MurNAc-L-Ala (UMA), the D-Glu moiety is often an important part of MurD inhibitors. For instance, phosphinates[17,18] and sulfonamides[15,16] bearing a D-Glu moiety have been designed as tetrahedral transition state or product analogue inhibitors. MurD inhibitors have also been identified by virtual screening,[19,20] by de novo structure-based drug design,[21] by screening phage display libraries,[22] and by a new high-throughput fluorimetric assay.[23] Although several inhibitors of Mur ligases have been reported by other research groups, many of them lack antibacterial activity and none have been introduced to the clinic.[7,8,24]

Recently, we reported several series of Mur inhibitors, including multitarget inhibitors of Mur ligases[25,26] and a series of MurD-selective inhibitors represented by the most potent compounds **I** and **II** (Figure 1).[27,28] The design of MurD inhibitors combining the D-Glu moiety and the thiazolidin-4-one ring was guided by the highest ranked quinazoline-based compound in virtual screening.[27] Using structure-based design, through several structure optimization cycles, we increased the MurD inhibitory potency of this type of inhibitor up to 45 μM (compound **II**, Figure 1).[28] The crystal structure of the MurD−**I** complex revealed that these inhibitors act as MurD product analogues, since the D-Glu moiety is seen to occupy the D-Glu-binding pocket and the thiazolidine-2,4-dione ring binds into the uracil-binding pocket.[28]

In the present study, starting from **I** and **II**, we report the design, synthesis, biological evaluation, and binding mode studies of a new series of structurally optimized, D-Glu-based potent MurD inhibitors containing the thiazolidin-4-one ring or its surrogates. On the basis of the crystal structure of the MurD−**I** complex and supported by ligand docking studies using GOLD 4.1,[29] we examined the effects on MurD inhibitory activity of different structural modifications of the parent compounds **I** and **II**, including (i) addition of a fluorine or hydroxyl group to ring A (compounds **15**−**17**), (ii) replacement of the thiazolidine-2,4-dione or rhodanine ring by pseudothiohydantoin, hydantoin, cinnamic, and acetic acid moieties (compounds **28**, **29**, **34**, **40**, **45**, and **54**), (iii) replacement of the methyleneamino linker between rings A and B by aminomethylene (compound **61**), and (iv) introduction of substituents with acidic character on the linker amino group (compounds **70**−**75**) in both the rhodanine- and thiazolidine-2,4-dione-based analogues. These efforts resulted in novel MurD inhibitors with improved potency, some of which displayed weak antibacterial activity. In addition, we present the crystal structure of a novel inhibitor **16** in complex with MurD that reveals additional information on the binding mode of the 5-benzylidenethiazolidin-4-one class of MurD inhibitors and served in this work as a foundation for structure-based design of compounds with improved potency against

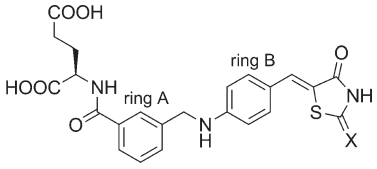

I, X=O IC_{50} (MurD) = 85 μM
II, X=S IC_{50} (MurD) = 45 μM

Figure 1. Thiazolidine-2,4-dione- and rhodanine-based MurD inhibitors **I** and **II**.[28]

MurD. Moreover, the crystal structures of the representative glutamic acid-based inhibitors **I** and **16**, incorporating thiazolidine-2,4-dione and rhodanine moieties, in complex with MurD, support the specific action of this structural type of MurD inhibitors, since 5-benzylidenerhodanines have recently been presented as pan assay interference compounds (PAINS), especially in screening-based research. They were recognized as frequent hitters that can covalently modify proteins by acting as Michael acceptors and often represent false positive hits in a variety of assays.[30−32]

2. RESULTS AND DISCUSSION

2.1. Design. The crystal structure of MurD in complex with thiazolidine-2,4-dione-based inhibitor **I** shows that the D-Glu moiety that occupies the D-Glu-binding pocket, and the heterocyclic ring that binds into the uracil-binding pocket form the majority of hydrogen bonds with MurD active site residues, while the linker between these two structural elements is involved mainly in hydrophobic interactions and hydrogen-bonds to the protein through crystal water molecules.[28] The design of the new series of MurD inhibitors was guided by information obtained from this crystal structure and was supported by ligand docking, using GOLD 4.1,[29] into the MurD active site.

Given the importance of the D-Glu moiety for MurD inhibition, we left this part of the molecule unchanged and, in the first step, modified phenyl ring A by introducing a fluorine or hydroxyl group in order to achieve additional interactions with the protein. Larger substituents on phenyl ring A have not been considered, since our docking calculations showed that incorporation of larger groups on ring A resulted in a different binding mode than that of the parent compounds. Candidates for the synthesis (compounds **15**−**17**, Scheme 1) had similar binding modes and gave comparable or better scores according to GOLDscore[33] than the parent compounds. Although the experimentally determined binding of **16** in the MurD active site showed a similar binding mode to that of the parent compound **II** (described below), the MurD inhibitory activity was weaker. Since introduction of additional groups in ring A resulted in different positioning of the part of the molecule between the D-Glu and the rhodanine ring (which was apparently the cause of the weaker activity against MurD), we decided to retain the unsubstituted 1,3-phenylene ring A, present in parent compounds **I** and **II**, as a building block for the newly designed compounds.

In the next step, we studied the replacement of the rhodanine or thiazolidine-2,4-dione ring by the pseudothiohydantoin and hydantoin rings (compounds **28** and **29**, Scheme 2) that have similar potential for forming the hydrogen bond between O^{γ} of Thr36 and the NH group at position

Scheme 1. Synthesis of 5-Benzylidenerhodanine and 5-Benzylidenethiazolidine-2,4-dione Derivatives 15−17 Substituted on Ring A[a]

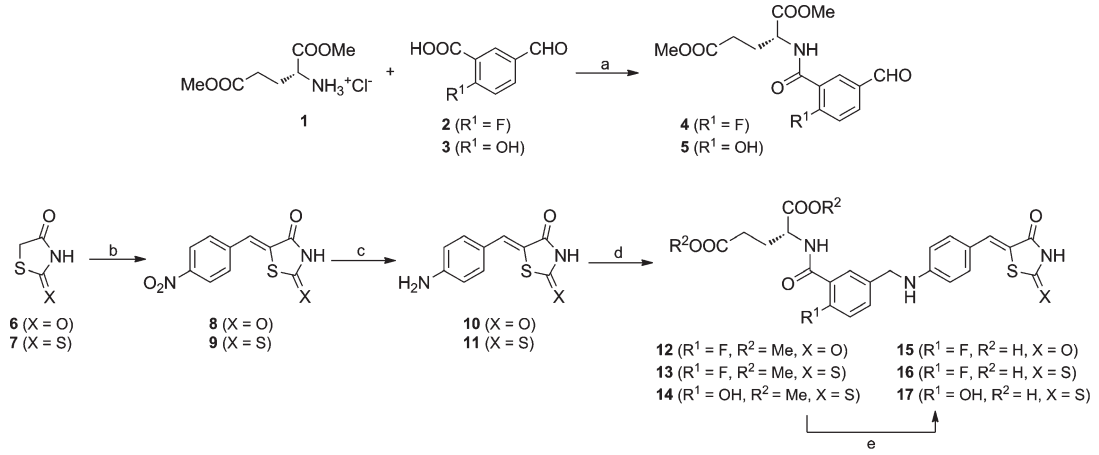

[a] Reagents and conditions: (a) TBTU, Et_3N, CH_2Cl_2, room temp, 3 h; (b) 4-nitrobenzaldehyde, piperidine, AcOH, EtOH, microwave 150 °C, 20 min; (c) $SnCl_2 \cdot 2H_2O$, EtOH, reflux, 2 h; (d) **4** or **5**, $NaCNBH_3$, AcOH, MeOH, room temp, 24 h; (e) 2 M LiOH, MeOH/H_2O, room temp, 16 h.

Scheme 2. Synthesis of 5-Benzylidenepseudothiohydantoin and 5-Benzylidenehydantoin Derivatives 28 and 29[a]

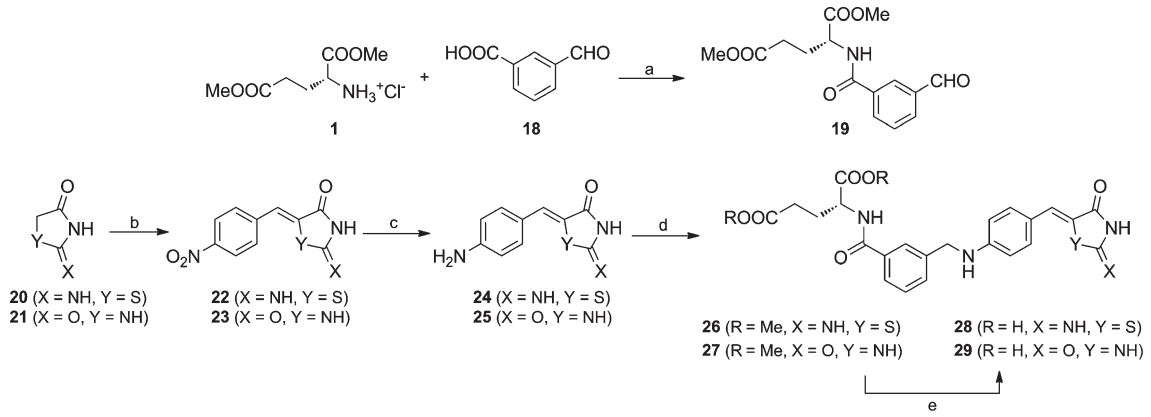

[a] Reagents and conditions: (a) TBTU, Et_3N, CH_2Cl_2, room temp, 3 h. (b) For the preparation of **22**: 4-nitrobenzaldehyde, NaOAc, AcOH, reflux, 20 h. For the preparation of **23**: 4-nitrobenzaldehyde, NH_4OAc, AcOH, reflux, 20 h. (c) For the preparation of **24**: $SnCl_2 \cdot 2H_2O$, EtOH, reflux, 2 h. For the preparation of **25**: H_2, Pd/C, THF/DMF, room temp, 20 h. (d) For the preparation of **26**: **19**, $Na(OAc)_3BH$, CF_3COOH, CH_2Cl_2, room temp, 20 h. For the preparation of **27**: **19**, $NaCNBH_3$, AcOH, MeOH, room temp, 20 h. (e) 2 M LiOH, MeOH/H_2O, room temp, 16 h.

3 of the thiazolidine-2,4-dione ring observed in the crystal structure of the MurD−**I** complex.[28] Further, as an acyclic mimetic of the thiazolidin-4-one ring, the carboxylic acid moiety was considered (cf. cinnamic acid derivative **34** and phenoxyacetic acid analogues **40** and **45**, Scheme 3). While cinnamic acid derivative **34** is conformationally rigid, since it retains conjugation between the phenyl ring and the carbonyl of the carboxylate group through the double bond, the phenoxyacetic acid derivatives **40** and **45** can be treated as flexible unconjugated analogues of **34**. A similar approach was used in the case of 5-benzylthiazolidine-2,4-dione-based PPARγ ligands, such as rosiglitazone, where the thiazolidine-2,4-dione ring was replaced by the 2-hydroxy-3-phenylpropanoic acid moiety, e.g., in aleglitazar.[34,35] The retained formation of the hydrogen bond, observed between the NH group of the thiazolidine-2,4-dione ring or the carboxylate group of the propanoic acid moiety and the OH group of Tyr473 in PPARγ-rosiglitazone and PPARγ-aleglitazar complexes, respectively, makes acyclic carboxylic acids interesting thiazolidin-4-one ring surrogates. Since, with introduction of the phenoxyacetic acid moiety in our MurD inhibitors, the number of rotatable bonds is increased, the central part of the inhibitor was rigidified by cyclization to the indole ring (compound **54**, Scheme 4). In addition to this change, in the case of the indole-based compound **54**, we have also replaced the methyleneamino linker between phenyl rings A and B by an aminomethylene group, which was also considered in compound **61** (Scheme 5). Docking the designed compounds **28**, **29**, **34**, **40**, **45**, **54**, and **61** in the MurD active site (Supporting Information Figure S2) showed the expected binding modes, similar to that of the parent compound **I**, and supported the decision to synthesize these potential MurD inhibitors.

The diphosphate-MurNAc part of the UMAG molecule forms several interactions with MurD active site residues.[9] However, superposition of the UMAG molecule and the thiazolidin-4-one-

dx.doi.org/10.1021/jm2002525 |J. Med. Chem. 2011, 54, 4600–4610

Scheme 3. Synthesis of Cinnamic and Acetic Acid Derivatives 34, 40, and 45[a]

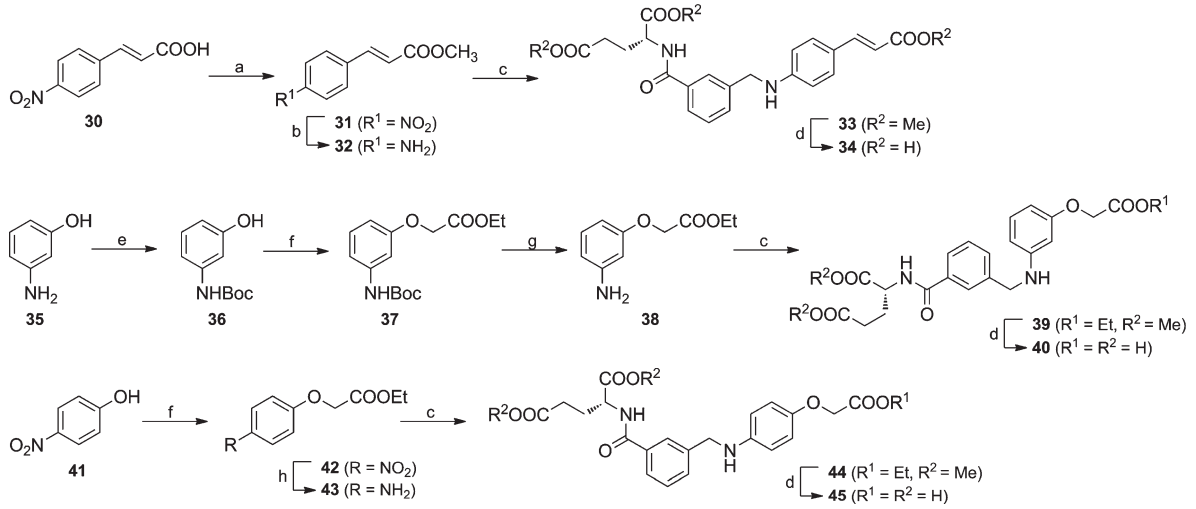

[a] Reagents and conditions: (a) $SOCl_2$, MeOH, room temp, 40 h; (b) $SnCl_2 \cdot 2H_2O$, EtOH, reflux, 2 h; (c) **19**, $Na(OAc)_3BH$, AcOH, THF, room temp, 20 h; (d) 2 M LiOH, $MeOH/H_2O$, room temp, 16 h; (e) $(Boc)_2O$, 1,4-dioxane, room temp, 16 h; (f) ethyl bromoacetate, K_2CO_3, CH_3CN, 60 °C, 18 h; (g) CF_3COOH, CH_2Cl_2, room temp, 1 h; (h) H_2, Pd/C, THF/EtOH, room temp, 4 h.

Scheme 4. Synthesis of Indole Core Containing Acetic Acid Derivative 54[a]

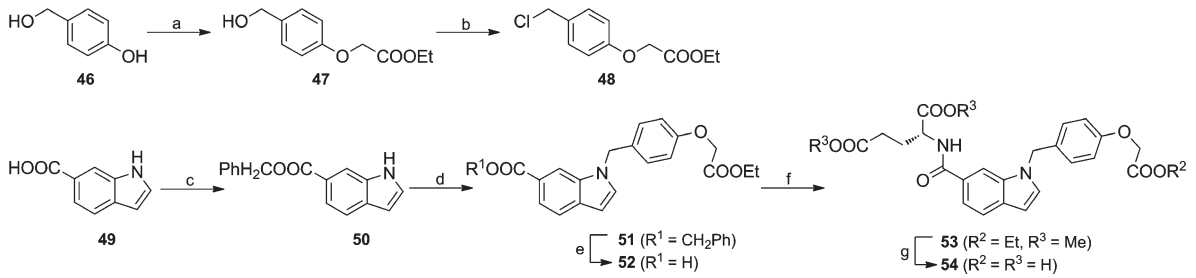

[a] Reagents and conditions: (a) ethyl bromoacetate, K_2CO_3, CH_3CN, 60 °C, 18 h; (b) $SOCl_2$, DMF, CH_2Cl_2, 0 °C, 45 min; (c) benzyl bromide, DBU, DMF, room temp, 15 h; (d) **48**, NaH, DMF, room temp, 18 h; (e) H_2, Pd/C, THF, room temp, 1 h; (f) H-D-Glu(OMe)-OMe·HCl, TBTU, Et_3N, CH_2Cl_2, room temp, 5 h; (g) 2 M LiOH, $MeOH/H_2O$, room temp, 16 h.

Scheme 5. Synthesis of Derivative 61 with an Aminomethylene Linker between Rings A and B[a]

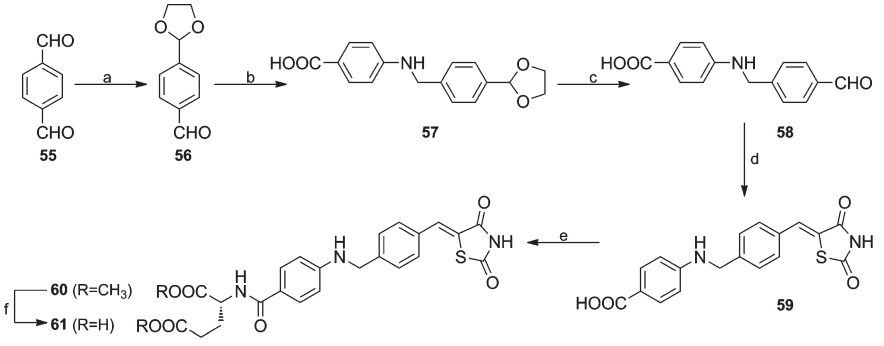

[a] Reagents and conditions: (a) ethylene glycol, *p*-toluenesulfonic acid, benzene, reflux, 24 h; (b) 4-aminobenzoic acid, $NaCNBH_3$, MeOH, room temp, 16 h; (c) 1 M HCl, THF/H_2O, room temp, 18 h; (d) thiazolidine-2,4-dione, piperidine, AcOH, EtOH, reflux, 24 h; (e) H-D-Glu(OMe)-OMe·HCl, TBTU, Et_3N, CH_2Cl_2, room temp, 5 h; (f) 2 M LiOH, $MeOH/H_2O$, room temp, 16 h.

based inhibitors in the MurD active site reveals that the diphosphate-MurNAc binding site is not occupied by the inhibitors, thus providing the potential for additional interactions with the active site residues that could improve the inhibitory potency of the parent compounds **I** and **II**. Because of the acidic character of the diphosphate moiety of UMAG, we have introduced negatively charged oxalyl, malonyl, and succinyl moieties on the amino group between rings A and B (compounds **70**–**75**,

dx.doi.org/10.1021/jm2002525 |*J. Med. Chem.* 2011, 54, 4600–4610

Scheme 6. Synthesis of N-Acylated Compounds 70−75[a]

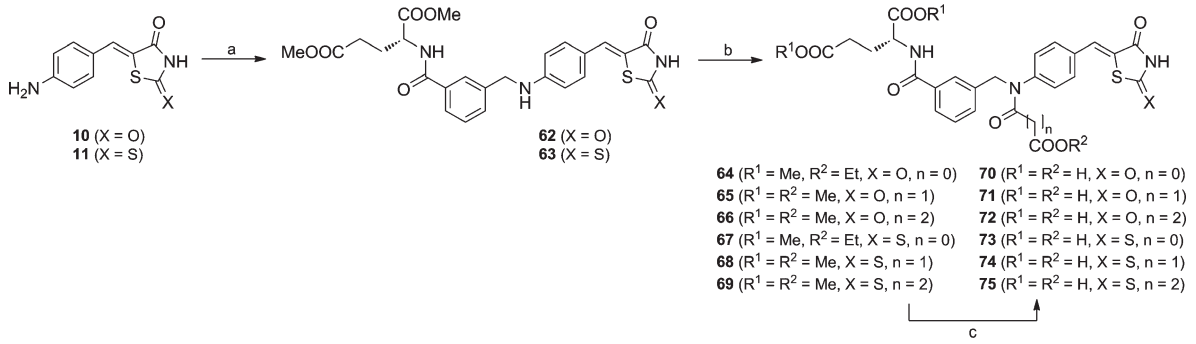

[a] Reagents and conditions: (a) **19**, $NaCNBH_3$, AcOH, MeOH, room temp, 20 h. (b) For the preparation of **64** and **67**: ethyl oxalyl chloride, Et_3N, DMF, room temp, 24 h. For the preparation of **65** and **68**: methyl malonyl chloride, Et_3N, DMF, room temp, 24 h. For the preparation of **66** and **69**: methyl succinyl chloride, Et_3N, DMF, room temp, 24 h. (c) 2 M LiOH, MeOH/H_2O, room temp, 16 h.

Scheme 6) to explore the diphosphate-binding pocket and to try to improve MurD inhibition by gaining additional interactions with the active site residues.

2.2. Chemistry. The syntheses of target compounds **15**−**17** with fluorine or a hydroxyl group on the phenyl ring A are outlined in Scheme 1. In the first step, 5-(4-nitrobenzylidene)thiazolidine-2,4-dione (**8**) and 5-(4-nitrobenzylidene)rhodanine (**9**) were synthesized via Knoevenagel condensation between 4-nitrobenzaldehyde and thiazolidine-2,4-dione (**6**) or rhodanine (**7**), using microwave irradiation with glacial acetic acid and piperidine as catalysts. The presence of only one signal in the ^{1}H NMR spectra for the methyne proton at 7.90 and 7.74 ppm, respectively, suggested, according to previous studies, exclusive formation of the thermodynamically stable *Z*-isomer.[36,37] Reduction of the nitro group in **8** and **9** with tin(II) chloride dihydrate gave amines **10** and **11** which, after reductive amination with benzaldehydes **4** or **5** using sodium cyanoborohydride, produced secondary amines **12**−**14**. Benzaldehydes **4** and **5** had been synthesized using TBTU-promoted coupling of D-glutamic acid dimethyl ester (**1**) with benzaldehyde **2** or **3**. Finally, target compounds **15**−**17** were obtained after alkaline hydrolysis of dimethyl esters **12**−**14** with aqueous lithium hydroxide.

The synthesis of compounds **28** and **29** incorporating pseudothiohydantoin (**20**) and hydantoin (**21**) rings instead of the thiazolidine-2,4-dione or rhodanine heterocycle is shown in Scheme 2. First, 5-(4-nitrobenzylidene)pseudothiohydantoin (**22**) and 5-(4-nitrobenzylidene)hydantoin (**23**) were obtained via Knoevenagel condensation of 4-nitrobenzaldehyde with **20** or **21** using sodium or ammonium acetate as catalyst. Aromatic amines **24** and **25** were synthesized by reduction of **22** with tin(II) chloride dihydrate and by catalytic hydrogenation of **23**, respectively. In the next step, reductive amination of **24** or **25** with benzaldehyde **19**, synthesized from **1** and **18**, gave compounds **26** and **27**. Because of the very poor reactivity of **24**, an alternative method for reductive amination was necessary to obtain **26**. In this case, sodium triacetoxyborohydride in trifluoroacetic acid was used to yield **26** in reasonable yield.[38] Pseudothiohydantoin- and hydantoin-based analogues **28** and **29** were obtained after alkaline hydrolysis of methyl esters **26** and **27**, using an aqueous solution of lithium hydroxide.

The syntheses of compounds possessing cinnamic and acetic acid moieties (**34**, **40**, **45**, and **54**) are outlined in Schemes 3 and 4. 4-Nitrocinnamic acid (**30**) was first protected as methyl ester **31** and then reduced using tin(II) chloride dihydrate to afford amine **32**. Compound **33** was obtained by sodium triacetoxyborohydride promoted reductive amination of **32** with aldehyde **19** and, in the following step, hydrolyzed with aqueous lithium hydroxide to yield target compound **34**. Acetic acid derivatives **40** and **45** were synthesized using slightly modified synthetic procedures because of the different starting materials. In the case of **40**, the amino group of 3-aminophenol (**35**) was first protected as *tert*-butyl carbamate **36**, which was then alkylated using ethyl bromoacetate and potassium carbonate to yield **37**. The latter was deprotected with acidolysis using trifluoroacetic acid to yield **38** which, after reductive amination with aldehyde **19** followed by alkaline hydrolysis of the obtained **39**, gave target compound **40**. For the synthesis of **45**, 4-nitrophenol (**41**) was first alkylated with ethyl bromoacetate and the resulting intermediate **42** hydrogenated to aromatic amine **43**. Target compound **45** was then obtained from **43** using the same synthetic strategy as described for **40**. Indole derivative **54** was synthesized starting from commercially available indole-6-carboxylic acid (**49**) that was first protected as benzyl ester **50** using benzyl bromide and DBU. N-Alkylation of indole **50** with benzyl chloride **48**, using sodium hydride as a base, gave **51**. Compound **48** had been obtained from 4-hydroxybenzyl alcohol (**46**) after alkylation with ethyl bromoacetate, followed by nucleophilic substitution of the hydroxyl group in **47** by chlorine using thionyl chloride and a catalytic amount of *N*,*N*-dimethylformamide.[39] Catalytic hydrogenation of **51** resulted in the deprotection of the benzyl ester moiety. The resulting carboxylic acid **52** was converted to D-Glu derivative **53** using TBTU-promoted coupling with the dimethyl ester of D-Glu (**1**). The final compound **54** was obtained by alkaline hydrolysis of **53** with aqueous lithium hydroxide.

Compound **61**, which possesses an aminomethylene linker between phenyl rings A and B, was synthesized as described in Scheme 5. In the first step, terephthalaldehyde (**55**) was monoprotected with ethylene glycol, using *p*-toluenesulfonic acid as catalyst, to give the aldehyde **56**. Reductive amination of aldehyde **56** with 4-aminobenzoic acid afforded intermediate **57** which, after deprotection using 1 M hydrochloric acid, gave aldehyde **58**. 5-Benzylidenethiazolidine-2,4-dione derivative **59** was then prepared via a Knoevenagel condensation between aldehyde **58** and thiazolidine-2,4-dione (**6**). The presence of only one signal for the methyne proton at 7.77 ppm in the ^{1}H NMR spectrum again suggested the formation of only the *Z* isomer. The target compound **61** was obtained after alkaline hydrolysis of

dx.doi.org/10.1021/jm2002525 |*J. Med. Chem.* 2011, 54, 4600–4610

Table 1. Inhibitory Activities of Compounds 15−17, 28, 29, 34, 40, 45, 54, 61, and 70−75 against MurD ligase from *E. coli*

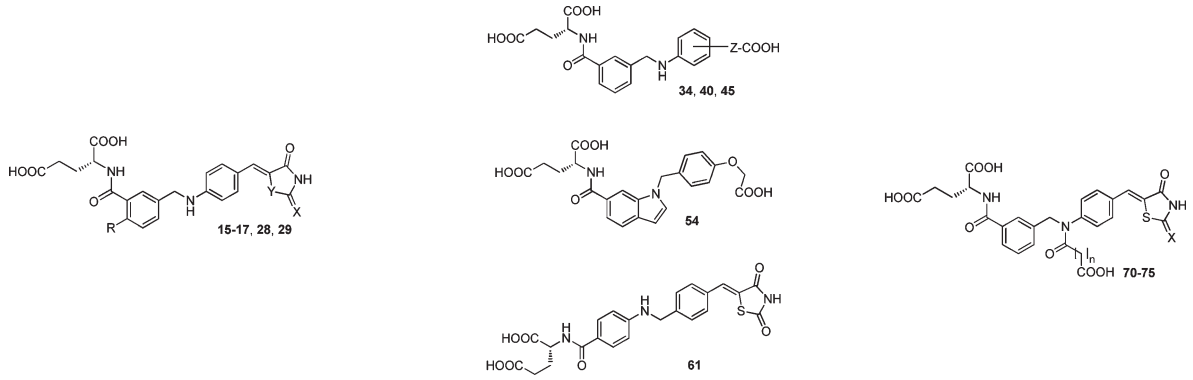

compd	X	Y	R	MurD RA[a] or IC_{50} [b]	compd	substitution	Z	MurD RA,[a] %	compd	X	*n*	MurD IC_{50},[b] μM
15	O	S	F	71%	**34**	1,4	CH=CH	96	**70**	O	0	40 ± 1
16	S	S	F	253 ± 27 μM	**40**	1,3	OCH_2	89	**71**	O	1	15 ± 2
17	S	S	OH	124 ± 3 μM	**45**	1,4	OCH_2	87	**72**	O	2	105 ± 4
28	NH	S	H	85%	**54**			94	**73**	S	0	5 ± 0.4
29	O	NH	H	99%	**61**			88	**74**	S	1	3 ± 0.3
									75	S	2	7 ± 0.2

[a] Residual activity (in %) of the enzyme at 500 μM tested compound. Results are the mean of two independent experiments. Standard deviations were within ±10% of the mean. [b] Concentration of the inhibitor, where residual activity of the enzyme is 50%.

60, which was prepared via TBTU-promoted amide bond formation between **59** and D-glutamic acid dimethyl ester hydrochloride (**1**).

N-Acyl derivatives **70**−**75** were synthesized as outlined in Scheme 6. Compounds **62** and **63**, prepared from **10** or **11** and **19** as reported previously,[28] were acylated using an excess of ethyl oxalyl chloride, methyl malonyl chloride or methyl succinyl chloride and triethylamine, to yield **64**−**69**. Finally, alkaline hydrolysis of **64**−**69** with aqueous lithium hydroxide gave compounds **70**−**75**.

2.3. Biological Activity. Target compounds **15**−**17**, **28**, **29**, **34**, **40**, **45**, **54**, **61**, and **70**−**75** were assayed for inhibition of MurD ligase from *E. coli* (Table 1). The Malachite green assay,[40] which detects orthophosphate generated during the enzymatic reaction, was used. All compounds were tested in the presence of detergent (0.01% Triton X-100) to avoid nonspecific inhibition due to aggregate formation.[41] The results are presented as residual activities (RAs) of the enzyme in the presence of 500 μM of each compound and as IC_{50} values for the most active compounds. They show that incorporation of the fluorine or hydroxyl group in ring A reduces MurD inhibition. The thiazolidine-2,4-dione-based compound **15** (RA = 71%) had almost none of the MurD inhibitory activity of the parent compound **I** (IC_{50} = 85 μM); that of the rhodanine-based compound **16**, with an IC_{50} of 253 μM, was more than 5-fold weaker than that of compound **II** (IC_{50} = 45 μM). A comparison of the position of ring A in the MurD active site of the crystal structures of MurD−**I** and MurD−**16** complexes shows that the introduction of fluorine results in different orientations of ring A (see below). The hydroxyl-substituted compound **17** with IC_{50} of 124 μM was almost 3-fold less potent than **II**, but the effect of the hydroxyl group was less detrimental to the MurD inhibitory activity than that of the fluorine atom. Pseudothiohydantoin- (**28**), hydantoin- (**29**), cinnamic acid- (**34**), acetic acid- (**40** and **45**), and the rigidified indole- (**54**) based compounds were all devoid of MurD inhibitory activity, which indicates that the rhodanine and thiazolidine-2,4-dione surrogates introduced are not favorable for binding to the uracil-binding pocket of the MurD active site. The lack of activity of compounds **40**, **45**, and **54** could be attributed to greater flexibility of the phenoxyacetic acid moiety of the molecules, compared to the 5-benzylidenethiazolidin-4-one moiety and/or to the loss of conjugation, which has been observed for reduced analogues of **I** and **II** and for compounds with flexible alkyl linkers replacing the benzylamine moiety.[28] Thiazolidine-2,4-dione **61** with 1,4-substitution on the two phenyl rings also proved to be inactive against MurD ligase, which further supports the necessity of the 1,3-substitution pattern in ring A for achieving potent MurD inhibition.[28] Finally, introduction of carboxylate-containing acyl substituents, such as oxalyl, malonyl, and succinyl groups, on the amino group between rings A and B resulted in the most potent series of MurD inhibitors, with IC_{50} values down to 3 μM. In general, rhodanine-based compounds **73**−**75** were an order of magnitude better than the thiazolidine-2,4-dione-based compounds **70**−**72**. This observation is consistent with our previous results showing that the rhodanine-based compound **II** and its analogues were usually more potent than their thiazolidine-2,4-dione-based counterparts, such as **I**.[28] MurD inhibition by thiazolidine-2,4-diones **70**−**72** was dependent mainly on the chain length of the *N*-acyl substituent. Compound **71**, with a malonyl group, was the most potent in the series, with an IC_{50} of 15 μM, followed by oxalyl-substituted compound **70** with an IC_{50} of 40 μM. The weakest inhibitor was compound **72**, with a succinyl moiety, which had an IC_{50} of 105 μM. The same trend is also seen in the rhodanine series that exhibited IC_{50} values of 5 μM (**73**), 3 μM (**74**) and 7 μM (**75**), confirming the malonyl moiety as the optimal chain length.

MurD ligase inhibitors **74** and **75** were tested for their antibacterial activity against two Gram-positive (*S. aureus* ATCC 29213, *E. faecalis* ATCC 29212) and two Gram-negative (*E. coli* ATCC 25922, *Pseudomonas aeruginosa* ATCC 27853)

dx.doi.org/10.1021/jm2002525 |*J. Med. Chem.* 2011, 54, 4600–4610

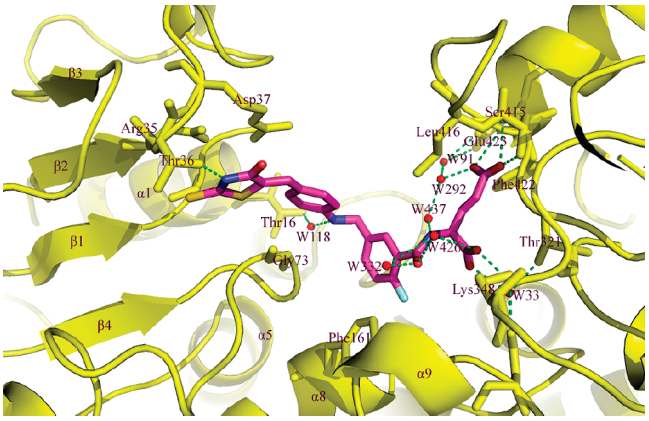

Figure 2. X-ray binding mode of inhibitor **16** (in magenta) in the active site of MurD from *E. coli* (PDB entry 2Y68). Hydrogen bonds between **16** and MurD active site residues (in yellow) and crystal water molecules (in red) are presented as dashed green lines.

bacteria. Compound **74** was found to inhibit *E. faecalis* growth weakly, with an MIC of 128 μg/mL, while compound **75** inhibited the growth of both Gram-positive bacteria with an MIC of 128 μg/mL. Additionally, esters **68** and **69** were tested as their potential prodrugs with better potential for entry into the bacterial cell but were found to be inactive against all four bacterial strains. All compounds were inactive against both Gram-negative bacteria.

2.4. X-ray Crystallography. The binding mode of inhibitor **16** in the MurD active site was determined by solving the crystal structure of the MurD−**16** complex (PDB entry 2Y68). Apo-MurD[13] was employed as a search model in a molecular replacement experiment (Figure 2 and Figure S1 in the Supporting Information). The crystal structure, solved to 1.5 Å, shows that the inhibitor occupies the binding site of the MurD product UMAG, which has already been observed in the case of a previously reported thiazolidine-2,4-dione-based inhibitor **I**.[28] The D-Glu moiety of the inhibitor in the MurD−**16** complex occupies the same site as the D-Glu residue of the product UMAG.[9] The α-carboxyl group of the D-Glu moiety of inhibitor **16** forms a charge-based interaction with N^{ξ} of Lys348 and is additionally hydrogen-bonded to a conserved water molecule W33 that is further hydrogen-bonded to O^{γ} of Thr321 and to the carboxyl group of Asp182. The carboxyl group of the D-Glu side chain is held in place by hydrogen bonds with O^{γ} and N^{α} of Ser415 and also with the backbone nitrogen of Phe422 and W292; the latter further interacts, via W91, with the side chain carboxyl group of Glu423. Water molecule W292 also forms a hydrogen bond with water molecule W437, which is in direct contact with the amide nitrogen of the D-Glu moiety of the inhibitor, forming an extended ring-type system. The carbonyl oxygen in the amide bond between D-Glu and ring A is hydrogen-bonded to W332 which, through W426, is in contact with the α-carboxyl group of the inhibitor. Additional interactions between the amino group in the para position of the 5-benzylidenerhodanine ring and W118, the latter being hydrogen-bonded to O^{γ} of Thr16, also contribute to the recognition within the active site. The aminobenzylidene moiety is held in place by hydrophobic interactions with Gly73, while the phenyl ring A is similarly held in place by hydrophobic interactions with Leu416 and by $\pi-\pi$ interactions with Phe161. Introduction of fluorine that, contrary to our expectations, does not interact with the enzyme active site residues results in a different position of phenyl ring A, which is rotated by 48° relative to ring A of **I** in the MurD−**I** complex. In the MurD−**16** complex, the uracil-binding pocket is occupied by the rhodanine ring of the inhibitor, the rhodanine ring participating in interplane stacking, with a salt bridge between Asp35 and Arg37. The ring nitrogen forms a hydrogen bond with the O^{γ} of Thr36. However, the hydrogen bond between Thr36 and the inhibitor oxo group, as formed in the MurD−**I** complex, is not observed in the MurD−**16** complex, which may, together with the different ring A position, account for the weaker MurD inhibitory potency of **16** with respect to **I**. The crystal structure of compound **16** in complex with MurD also provides evidence that the exocyclic double bond exists in the *Z*-configuration.

2.5. Molecular Docking. Plausible binding modes of target compounds **15**, **17**, **28**, **29**, **34**, **40**, **45**, **54**, **61**, and **70**−**75** in the active site of *E. coli* MurD ligase were determined by ligand docking of the compounds using GOLD 4.1.[29] In the crystal structure of MurD−**I** complex (PDB entry 2X5O)[28] the active site was defined as the area within 10 Å from inhibitor **I**. First, the system was validated by redocking **I** in the defined active site. The program, in combination with the GOLDscore[33] scoring function, was able to reproduce the experimentally determined binding conformation of **I** with an all heavy atom rmsd of only 0.72 Å. After the cocrystal structure of MurD−**16** (PDB entry 2Y68) was obtained, a similar experiment was carried out by redocking **16** in the active site. The calculated rmsd value between the experimental and calculated binding conformation of **16** was 1.03 Å. These results confirm GOLD 4.1 with the use of GOLDscore as a suitable docking program for predicting the binding modes of the new compounds designed to target MurD.

Docking inhibitor **17** in the MurD active site shows a binding mode similar to that of **16** and **I** (Figure 3a). The calculated conformation of ring A in **17** is comparable to its conformation in **16**. The hydroxyl group on ring A is within hydrogen bonding distance of the His183 side chain, which may account for the better binding affinity of **17** than of **16**, while the observed conformation of the middle part of the inhibitor may be less favorable than in **I**. Docked conformations of oxalyl-substituted inhibitors **70** (Figure S2) and **73** (Figure 3b) show that the oxalyl group is oriented away from the diphosphate-binding pocket and forms a plausible hydrogen bond with the side chain of Asn138. This additional interaction may account for the better binding affinity of **70** and **73** than that of the parent compounds **I** and **II**. Compounds **71** (Figure S2) and **74** (Figure 3c), with the malonyl substituent on the amino group of the linker, exhibited the best inhibitory potencies in the two series of *N*-acyl derivatives, which may be attributed to the possible interaction of the carboxyl end of the malonyl moiety with the guanidine group of Arg37, a residue that interacts with the phosphate group of the UMAG molecule. However, the weaker inhibitory activity of **72** than of **I** on the one hand and the more potent activity of **75** (Figure 3d) than of **II** on the other cannot be rationalized by the docking results, since the terminal carboxylate of the succinyl group of both **72** (Figure S2) and **75** is within hydrogen bonding distance of the Thr16 side chain hydroxyl group. The predicted additional hydrogen bond with Thr16, which is also part of the diphosphate-binding pocket of UMAG, results in the stronger inhibition of MurD by **75**, but the less potent MurD inhibition by **72** may be attributed to conformational changes in other

dx.doi.org/10.1021/jm2002525 |*J. Med. Chem.* 2011, 54, 4600–4610

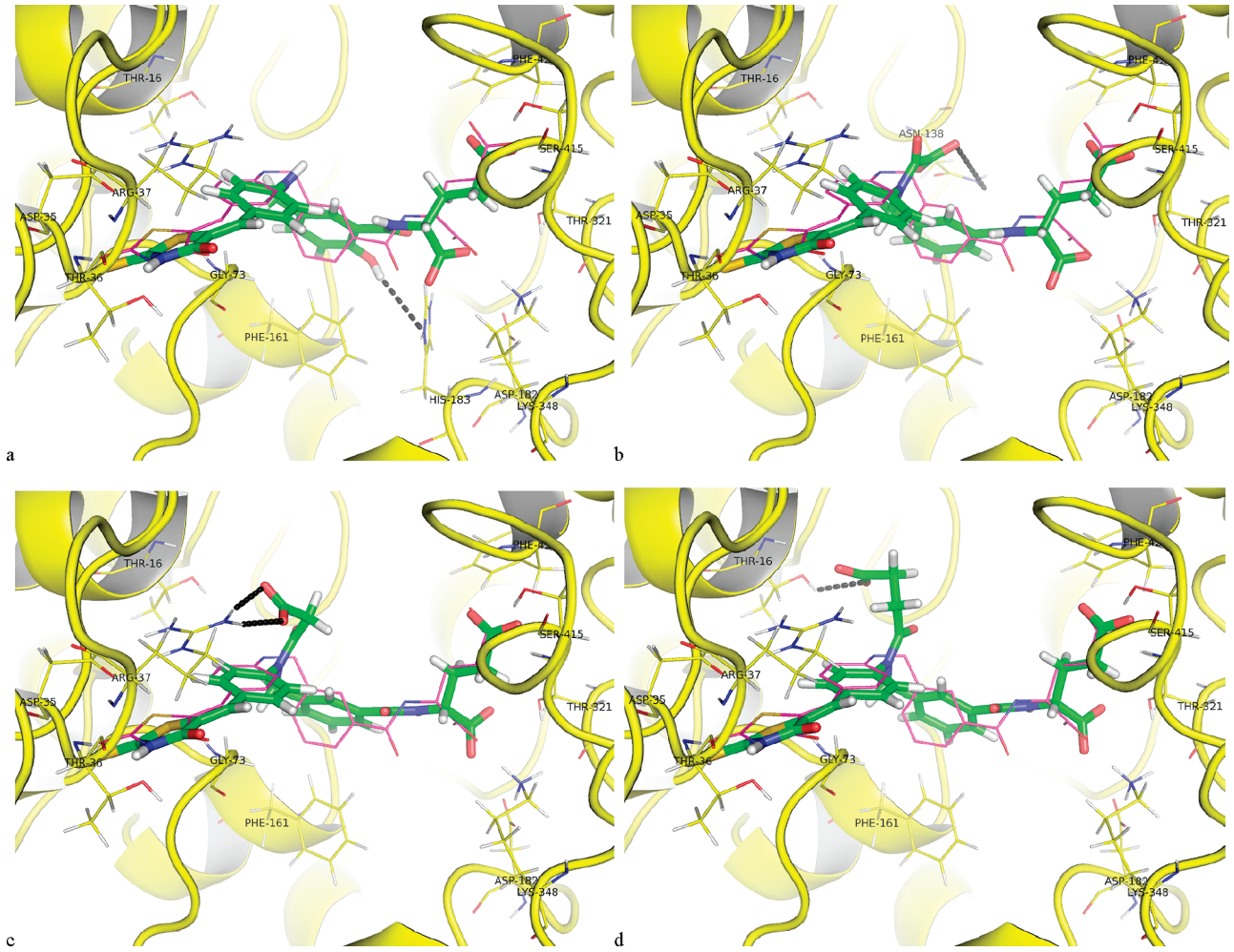

Figure 3. Superposition of inhibitor **I** (in magenta) and the best ranked GOLD-calculated conformation of inhibitor (in green): (a) **17**; (b) **73**; (c) **74**; (d) **75**. For clarity, only the amino acid residues interacting with inhibitor **I** (according to the crystal structure) and additional residues forming plausible hydrogen bonds (presented as black dashed lines) with oxalyl, malonyl, or succinyl carboxylate groups of **73**−**75** are shown.

parts of the molecule of **72**. Moreover, the difference in the potencies of thiazolidine-2,4-diones **70**−**72** compared to those of rhodanines **73**−**75** can also not be interpreted by the docking results.

3. CONCLUSION

We have designed, synthesized, and evaluated a series of novel D-glutamic acid-based inhibitors of *E. coli* MurD ligase that incorporate the 5-benzylidenethiazolidin-4-one moiety. They exhibit more potent inhibition than the parent compounds **I** and **II**. The crystal structure of MurD ligase in complex with **16** shows a binding mode slightly different from the previously determined binding for **I** in the MurD active site. Both crystal structures have served as a foundation for the structure-based design of the most potent series of MurD inhibitors **73**−**75**, which have acidic moieties attached to the amino group of the linker between the two phenyl rings. They inhibited MurD with IC_{50} values between 3 and 7 μM and showed weak antibacterial activity. Inhibition of MurD ligase in the low micromolar range makes compounds **73**−**75**, to the best of our knowledge, the most potent D-glutamic acid based MurD inhibitors reported to date.

4. EXPERIMENTAL SECTION

4.1. Molecular Docking. *4.1.1. Ligand and Protein Preparation.* Three-dimensional models of target compounds were built from a standard fragment library, and their geometries were optimized using the CHARMm force field[42] with MMFF94[43] partial atomic charges. The Smart Minimizer algorithm as available in Accelrys Discovery Studio 2.5,[44] running on a workstation with Intel Core i7 860 CPU processor, 8 GB RAM, two 750 GB hard drives and a Nvidia GT220 GPU graphic card, running Centos 5.5, was used for energy minimization until the gradient value was smaller than 0.001 kcal/(mol Å). Molecular docking calculations were performed using GOLD program, version 4.1.[29] 5-Benzylidenethiazolidine-2,4-dione-based inhibitor **I** and water molecules were deleted from the crystal structure of MurD−**I** complex (PDB code 2X5O), and hydrogen atoms were added to the protein using GOLD. The amino acid residues within a radius of 10 Å around the inhibitor were defined as the active site.

4.1.2. Docking Validation and Ligand Docking. In order to validate GOLD 4.1 as a suitable docking program, compound **I** was docked into the MurD active site (PDB code 2X5O)[28] in 100 independent genetic algorithm (GA) runs. The best ranked GOLD-calculated conformation of **I**, using GOLDscore as a scoring function, had an all heavy atom rmsd value of 0.72 Å compared to the experimentally determined conformation of **I** in MurD active site.

dx.doi.org/10.1021/jm2002525 |*J. Med. Chem.* 2011, 54, 4600–4610

The target compounds were docked in 100 independent GA runs. The GA parameters were set as suggested by GOLD 4.1. Ligands with rmsd value less than 1.5 Å were joined in clusters. Early termination was allowed if the top 10 solutions were within 1.0 Å of the rmsd value. GOLDscore[33] was used as scoring function. The 10 best ranked docking solutions were inspected visually, and the best ranked GOLD-calculated conformation was used for analysis and representation. The figures were prepared by Pymol.[45]

4.2. Chemistry. Chemicals were obtained from Acros, Aldrich Chemical Co., and Fluka and used without further purification. Analytical thin-layer chromatography was performed on silica gel Merck 60 F_{254} precoated plates (0.25 mm), using visualization with ultraviolet light, ninhydrin, and 2,4-dinitrophenylhydrazine. Flash column chromatography was carried out on silica gel 60 (particle size 0.040−0.063 mm; Merck, Germany). HPLC analyses were performed on an Agilent Technologies HP 1100 instrument with a G1365B UV−vis detector, a G1316A thermostat, and a G1313A autosampler, using a Phenomenex Luna C18 column (4.6 mm × 250 mm) at a flow rate of 1 mL/min. The eluant was a mixture of 0.1% TFA in water (A) and methanol (B). Gradient was 10% B to 80% B in 20 min. Melting points were determined on a Reichert hot stage microscope and are uncorrected. ^{1}H NMR and ^{13}C NMR spectra were recorded at 300 and 75 MHz on a Bruker AVANCE DPX300 spectrometer in CD_3OD, $CDCl_3$, or DMSO-d_6 solution, with TMS as the internal standard. Spectra were assigned using gradient COSY, HSQC, and ^{1}H-coupled ^{13}C NMR experiments. IR spectra were recorded on a Perkin-Elmer 1600 FT-IR spectrometer. Mass spectra were obtained using a VG-Analytical Autospec Q mass spectrometer. Optical rotations were measured on a Perkin-Elmer 241 MC polarimeter. The reported values for specific rotation are average values of 10 successive measurements, using an integration time of 5 s. Since compounds **16**, **17**, **61**−**63**, **73**, and **74** showed ellipticity and circular dichroism, their specific rotation values are not reported. Microanalyses were performed on a Perkin-Elmer C, H, N analyzer 240 C. Analyses indicated by the symbols of the elements were within 0.4% of the theoretical values. The purity of the tested compound was established to be ≥95%. Microwave-assisted reactions were performed using a focused microwave reactor (Discover, CEM Corporation, Matthews, NC). Reactions were carried out in septum-sealed glass vials (10 mL) which enable high-pressure reaction conditions (max 20 bar). The temperature of the reaction mixture was monitored using a calibrated infrared temperature controller mounted under the reaction vessel.

*Synthesis of Compounds **67**−**69**.* Compound **63**[28] (1 mmol) was dissolved in anhydrous tetrahydrofuran (10 mL) and triethylamine (10 mmol). The solution was cooled to 0 °C, and ethyl oxalyl chloride, methyl malonyl chloride, or methyl succinyl chloride (5 mmol) was added. The reaction mixture was stirred at room temperature for 18 h, and then the solvent was evaporated under reduced pressure. The oily residue was dissolved in ethyl acetate (30 mL) and successively washed with 10% aqueous citric acid solution (2 × 30 mL), saturated aqueous $NaHCO_3$ solution (2 × 30 mL), and brine (30 mL), dried over Na_2SO_4, filtered and the solvent evaporated under reduced pressure. The crude product was purified with flash column chromatography using dichloromethane/methanol (20:1) as eluent.

*(R,Z)-Dimethyl 2-(3-((2-Ethoxy-2-oxo-N-(4-((4-oxo-2-thioxothiazolidin-5-ylidene)methyl)phenyl)acetamido)methyl)benzamido)pentanedioate (**67**).* Yield 58%; red solid; mp 70−71 °C; $[\alpha]_D^{20}$ +5.3° (*c* 0.25, MeOH). IR (NaCl): ν = 3630, 3374, 3054, 2946, 2831, 1685, 1360, 1266, 1194, 1070, 1017, 964, 848, 742 cm^{-1}. ^{1}H NMR (DMSO-d_6): δ 0.93 (t, 3H, *J* = 7.0 Hz, $CH_2\underline{CH_3}$), 1.93−2.18 (m, 2H, $CH\underline{CH_2}CH_2$), 2.44 (t, 2H, *J* = 7.4 Hz, $CHCH_2\underline{CH_2}$), 3.58 (s, 3H, CH_3), 3.64 (s, 3H, CH_3), 4.03 (q, 2H, *J* = 7.0 Hz, $C\underline{H_2}CH_3$), 4.41−4.48 (m, 1H, $C\underline{H}CH_2CH_2$), 5.10 (s, 2H, CH_2N), 7.38−7.47 (m, 4H, 2 × Ar−H′, 2 × Ar−H), 7.61−7.63 (m, 3H, CH═C, 2 × Ar−H′), 7.73−7.79 (m, 2H, 2 × Ar−H), 8.75 (d, 1H, *J* = 7.4 Hz, CONH), 13.88 (br s, 1H, CONHCS) ppm. MS (ESI+): *m*/*z* (%) = 628 ([M + H]$^+$, 100). HRMS (ESI+): *m*/*z* [M + H]$^+$ calcd for $C_{29}H_{30}N_3O_9S_2$, 628.1423; found, 628.1420. Anal. ($C_{29}H_{29}N_3O_9S_2$) C, H, N.

*(R,Z)-Dimethyl 2-(3-((3-Methoxy-3-oxo-N-(4-((4-oxo-2-thioxothiazolidin-5-ylidene)methyl)phenyl)propanamido)methyl)benzamido)pentanedioate (**68**).* Yield: 28%; orange crystals; mp 80−81 °C; $[\alpha]_D^{20}$ +18.1° (*c* 0.12, MeOH). IR (KBr): ν = 3422, 2952, 2849, 1736, 1654, 1597, 1508, 1438, 1330, 1230, 1179, 1009, 840 cm^{-1}. ^{1}H NMR (DMSO-d_6): δ 1.96−2.18 (m, 2H, $CH\underline{CH_2}CH_2$), 2.44 (t, 2H, *J* = 7.5 Hz, $CHCH_2\underline{CH_2}$), 3.38 (s, 2H, $COCH_2\underline{CO}$), 3.57 (s, 3H, CH_3), 3.58 (s, 3H, CH_3), 3.64 (s, 3H, CH_3), 4.41−4.48 (m, 1H, $C\underline{H}CH_2CH_2$), 5.01 (s, 2H, CH_2N), 7.40−7.43 (m, 4H, 2 × Ar−H′, 2 × Ar−H), 7.60−7.63 (m, 3H, CH═C, 2 × Ar−H′), 7.70−7.77 (m, 2H, 2 × Ar−H), 8.70 (d, 1H, *J* = 7.5 Hz, CONH), 13.88 (br s, 1H, CONHCS) ppm. MS (ESI+): *m*/*z* (%) = 628 ([M + H]$^+$, 100). HRMS (ESI+): *m*/*z* [M + H]$^+$ calcd for $C_{29}H_{30}N_3O_9S_2$, 628.1423; found, 628.1438. Anal. ($C_{29}H_{29}N_3O_9S_2\cdot 0.6H_2O$) C, H, N.

*(R,Z)-Dimethyl 2-(3-((4-Methoxy-4-oxo-N-(4-((4-oxo-2-thioxothiazolidin-5-ylidene)methyl)phenyl)butanamido)methyl)benzamido)pentanedioate (**69**).* Yield: 43%; red oil; $[\alpha]_D^{20}$ +8.4 (*c* 0.16, MeOH). IR (NaCl): ν = 3650, 3340, 2945, 2832, 2577, 1831, 1741, 1602, 1361, 1268, 1196, 1023, 846, 740, 705 cm^{-1}. ^{1}H NMR (DMSO-d_6): δ 1.95−2.17 (m, 2H, $CH\underline{CH_2}CH_2$), 2.43 (t, 2H, *J* = 7.5 Hz, $CHCH_2\underline{CH_2}$), 3.56 (s, 3H, CH_3), 3.57 (s, 3H, CH_3), 3.59 (s, 2H, $COCH_2CH_2CO$), 3.61 (s, 2H, $COCH_2CH_2CO$), 3.63 (s, 3H, CH_3), 4.40−4.48 (m, 1H, $C\underline{H}CH_2CH_2$), 4.88−5.10 (m, 2H, CH_2N), 7.37−7.47 (m, 4H, 2 × Ar−H′, 2 × Ar−H), 7.61−7.77 (m, 5H, 2 × Ar−H′, CH═C, 2 × Ar−H), 8.68 (d, 1H, *J* = 7.5 Hz, CONH), 13.86 (br s, 1H, CONHCS) ppm. ^{13}C NMR ($CDCl_3$): δ 27.1, 27.4, 30.3, 33.2, 35.5, 52.0, 52.3, 52.6, 53.2, 126.7, 126.9, 129.1, 129.7, 130.9, 131.9, 133.3, 133.7, 137.2, 142.9, 167.1, 168.1, 168.7, 172.0, 172.4, 172.8, 173.6, 176.2, 193.1 ppm. MS (ESI+): *m*/*z* (%) = 642 ([M + H]$^+$, 100). HRMS (ESI+): *m*/*z* [M + H]$^+$ calcd for $C_{30}H_{32}N_3O_9S_2$, 642.1580; found, 642.1604.

*Synthesis of Compounds **73**−**75**.* To a stirred solution of dimethyl ester **67**−**69** (0.20 mmol) in MeOH/water (1:1) (10 mL), 2 M LiOH (1.40 mmol) was added, and the reaction mixture stirred overnight at room temperature. The solution was neutralized with 1 M HCl and concentrated under reduced pressure. The residual aqueous solution was acidified with 1 M HCl to pH 2 and the product extracted with ethyl acetate (3 × 15 mL). The combined organic phases were washed with brine (2 × 15 mL), dried over Na_2SO_4, filtered, and the solvent was evaporated under reduced pressure.

*(R,Z)-2-(3-((1-Carboxy-N-(4-((4-oxo-2-thioxothiazolidin-5-ylidene)-methyl)phenyl)formamido)methyl)benzamido)pentanedioic Acid (**73**).* The crude product was purified with flash column chromatography using dichloromethane/methanol/glacial acetic acid (12:1:1) as eluent. Yield: 51%; red solid; mp 140−142 °C. IR (KBr): ν = 3422, 1718, 1638, 1430, 1285, 1232, 1180, 1066, 1008, 901, 811 cm^{-1}. ^{1}H NMR (DMSO-d_6): δ 1.97−2.12 (m, 2H, $CH\underline{CH_2}CH_2$), 2.35 (t, 2H, *J* = 6.9 Hz, $CHCH_2\underline{CH_2}$), 4.34−4.41 (m, 1H, $C\underline{H}CH_2CH_2$), 5.08 (s, 2H, CH_2N), 7.36−7.45 (m, 4H, 2 × Ar−H′, 2 × Ar−H), 7.56−7.59 (m, 3H, CH═C, 2 × Ar−H′), 7.74−7.77 (m, 2H, 2 × Ar−H), 8.60 (d, 1H, *J* = 7.6 Hz, CONH), 12.23 (br s, 4H, CONHCS, 3 × COOH) ppm. ^{13}C NMR (CD_3OD): δ 20.8, 27.5, 31.5, 53.8, 128.0, 128.5, 128.6, 129.4, 130.0, 131.2, 132.5, 132.9, 134.4, 134.7, 135.7, 138.1, 170.1, 170.9, 174.9, 175.0, 175.3, 176.7, 196.3 ppm. MS (ESI+): *m*/*z* (%) = 572 ([M + H]$^+$, 100), 380 (57). HRMS (ESI+): *m*/*z* [M + H]$^+$ calcd for $C_{25}H_{22}N_3O_9S_2$, 572.0797; found, 572.0790. Anal. ($C_{25}H_{21}N_3O_9S_2\cdot 1.5H_2O\cdot 0.5CH_3COOH$) C, H, N.

*(R,Z)-2-(3-((2-Carboxy-N-(4-((4-oxo-2-thioxothiazolidin-5-ylidene)-methyl)phenyl)acetamido)methyl)benzamido)pentanedioic Acid (**74**).* The crude product was purified with flash column chromatography using dichloromethane/methanol/glacial acetic acid (12:1:0.5) as eluent. Yield 88%; orange crystals; mp 104−106 °C. IR (KBr): ν = 3420, 2927, 2076, 1718, 1636, 1596, 1508, 1418, 1231, 1180, 1116, 1011, 840 cm^{-1}. ^{1}H NMR (DMSO-d_6): δ 1.91−2.10 (m, 2H, $CH\underline{CH_2}CH_2$), 2.34 (t, 2H,

J = 7.1 Hz, $CHCH_2CH_2$), 3.28 (s, 2H, $COCH_2CO$), 4.38−4.42 (m, 1H, $CHCH_2CH_2$), 5.02 (s, 2H, CH_2N), 7.26−7.44 (m, 4H, 2 × Ar−H′, 2 × Ar−H), 7.60−7.74 (m, 5H, CH═C, 2 × Ar−H′, 2 × Ar−H), 8.55 (d, 1H, J = 7.6 Hz, CONH), 12.50 (br s, 3H, 3 × COOH), 13.86 (br s, 1H, CONHCS) ppm. ^{13}C NMR (CD_3OD): δ 20.8, 27.5, 31.5, 53.8, 68.2, 127.9, 128.4, 128.8, 129.6, 129.9, 130.4, 131.1, 132.3, 132.9, 135.5, 138.6, 144.3, 170.1, 170.2, 170.8, 171.0, 175.0, 176.6, 196.3 ppm. MS (ESI+): m/z (%) = 586 ($[M + H]^+$, 100). HRMS (ESI+): m/z $[M + H]^+$ calcd for $C_{26}H_{24}N_3O_9S_2$: 586.0954, found: 586.0947. HPLC t_R = 12.695 min (95.20% at 220 nm, 95.88% at 254 nm).

*(R,Z)-2-(3-((3-Carboxy-N-(4-((4-oxo-2-thioxothiazolidin-5-ylidene)-methyl)phenyl)propanamido)methyl)benzamido)pentanedioic Acid (**75**).* The crude product was purified with flash column chromatography using dichloromethane/methanol/glacial acetic acid (12:1:1) as eluent. Yield: 23%; orange solid; mp 133−135 °C; $[\alpha]_D^{20}$ −15.0° (c 0.15, DMF). IR (KBr): ν = 3422, 1718, 1635, 1406, 1229, 1178, 1010, 837, 747 cm^{-1}. ^{1}H NMR (DMSO-d_6): δ 1.91−2.12 (m, 2H, $CHCH_2CH_2$), 2.24−2.36 (m, 4H, $CHCH_2CH_2$, $NCOCH_2CH_2CO$), 2.58−2.86 (m, 2H, $NCOCH_2CH_2CO$), 4.34−4.41 (m, 1H, $CHCH_2CH_2$), 4.86−5.12 (m, 2H, CH_2N), 7.37−7.48 (m, 4H, 2 × Ar−H′, 2 × Ar−H), 7.51−7.77 (m, 4H, 2 × Ar−H′, CH═C, 2 × Ar−H), 8.52 (d, 1H, J = 7.7 Hz, CONH), 12.18 (br s, 4H, CONHCS, 3 × COOH) ppm. ^{13}C NMR (CD_3OD): δ 20.8, 27.8, 28.4, 31.6, 34.3, 54.1, 127.9, 128.2, 128.9, 129.9, 131.0, 131.1, 132.9, 133.8, 135.1, 135.6, 138.7, 144.1, 170.1, 170.6, 171.0, 175.7, 175.9, 176.8, 196.5 ppm. MS (ESI+): m/z (%) = 600 ($[M + H]^+$, 100). HRMS (ESI+): m/z $[M + H]^+$ calcd for $C_{27}H_{26}N_3O_9S_2$, 600.1110; found, 600.1099. HPLC t_R = 11.833 min (96.06% at 220 nm, 96.63% at 254 nm).

■ ASSOCIATED CONTENT

Supporting Information. Experimental procedures and characterization of intermediate and target compounds, results from microanalyses and HRMS, description of crystallization, preparation of the inhibitor complex, data collection, crystal structure solution, and model refinement, description of enzyme assay and determination of antibacterial activity. This material is available free of charge via the Internet at http://pubs.acs.org.

Accession Codes

[†]The PDB code for the Mur−**16** complex is 2Y68.

■ AUTHOR INFORMATION

Corresponding Author

*Phone: +386-1-4769635. Fax: +386-1-4258031. E-mail: lucija.peterlin@ffa.uni-lj.si.

■ ACKNOWLEDGMENT

This work was supported by the EU FP6 Integrated Project EUR-INTAFAR (Project No. LSHM-CT-2004-512138), by the Slovenian Research Agency (Grant No. P1-0208), and by the World Federation of Scientists. The authors thank Professor Roger Pain for critical reading of the manuscript.

■ ABBREVIATIONS USED

UDP, uridine 5′-diphosphate; UMA, UDP-*N*-acetylmuramoyl-L-Ala; UMAG, UDP-*N*-acetylmuramoyl-L-Ala-D-Glu; MurC, UDP-*N*-acetylmuramate:L-Ala ligase; MurD, UDP-*N*-acetylmuramoyl-L-Ala:D-Glu ligase; MurE, UDP-*N*-acetylmuramoyl-L-Ala-D-Glu: *meso*-diaminopimelate ligase; MurF, UDP-*N*-acetylmuramoyl-L-Ala-γ-D-Glu-*meso*-diaminopimelate:D-Ala-D-Ala ligase

■ REFERENCES

(1) Livermore, D. M. Bacterial resistance: origins, epidemiology, and impact. *Clin. Infect. Dis.* **2003**, *36*, 11–23.

(2) Chopra, I.; Schofield, C.; Everett, M.; O'Neill, A.; Miller, K.; Wilcox, M.; Frere, J. M.; Dawson, M.; Czaplewski, L.; Urleb, U.; Courvalin, P. Treatment of health-care-associated infections caused by Gram-negative bacteria: a consensus statement. *Lancet Infect. Dis.* **2008**, *8*, 133–139.

(3) Rice, L. B. Unmet medical needs in antibacterial therapy. *Biochem. Pharmacol.* **2006**, *71*, 991–5.

(4) Nordmann, P.; Naas, T.; Fortineau, N.; Poirel, L. Superbugs in the coming new decade; multidrug resistance and prospects for treatment of *Staphylococcus aureus*, *Enterococcus* spp. and *Pseudomonas aeruginosa* in 2010. *Curr. Opin. Microbiol.* **2007**, *10*, 436–440.

(5) Vollmer, W.; Blanot, D.; de Pedro, M. A. Peptidoglycan structure and architecture. *FEMS Microbiol. Rev.* **2008**, *32*, 149–167.

(6) van Heijenoort, J. Recent advances in the formation of the bacterial peptidoglycan monomer unit. *Nat. Prod. Rep.* **2001**, *18*, 503–519.

(7) Barreteau, H.; Kovač, A.; Boniface, A.; Sova, M.; Gobec, S.; Blanot, D. Cytoplasmic steps of peptidoglycan biosynthesis. *FEMS Microbiol. Rev.* **2008**, *32*, 168–207.

(8) El Zoeiby, A.; Sanschagrin, F.; Levesque, R. C. Structure and function of the Mur enzymes: development of novel inhibitors. *Mol. Microbiol.* **2003**, *47*, 1–12.

(9) Bertrand, J. A.; Auger, G.; Martin, L.; Fanchon, E.; Blanot, D.; Le Beller, D.; van Heijenoort, J.; Dideberg, O. Determination of the MurD mechanism through crystallographic analysis of enzyme complexes. *J. Mol. Biol.* **1999**, *289*, 579–590.

(10) Bouhss, A.; Dementin, S.; van Heijenoort, J.; Parquet, C.; Blanot, D. MurC and MurD synthetases of peptidoglycan biosynthesis: borohydride trapping of acyl-phosphate intermediates. *Methods Enzymol.* **2002**, *354*, 189–196.

(11) Emanuele, J. J.; Jin, H. Y.; Yanchunas, J.; Villafranca, J. J. Evaluation of the kinetic mechanism of *Escherichia coli* uridine diphosphate-*N*-acetylmuramate:L-alanine ligase. *Biochemistry* **1997**, *36*, 7264–7271.

(12) Anderson, M. S.; Eveland, S. S.; Onishi, H. R.; Pompliano, D. L. Kinetic mechanism of the *Escherichia coli* UDPMurNAc-tripeptide D-alanyl-D-alanine-adding enzyme: use of a glutathione *S*-transferase fusion. *Biochemistry* **1996**, *35*, 16264–16269.

(13) Bertrand, J. A.; Auger, G.; Fanchon, E.; Martin, L.; Blanot, D.; van Heijenoort, J.; Dideberg, O. Crystal structure of UDP-*N*-acetylmuramoyl-L-alanine:D-glutamate ligase from *Escherichia coli*. *EMBO J.* **1997**, *16*, 3416–3425.

(14) Bertrand, J. A.; Fanchon, E.; Martin, L.; Chantalat, L.; Auger, G.; Blanot, D.; van Heijenoort, J.; Dideberg, O. "Open" structures of MurD: domain movements and structural similarities with folylpolyglutamate synthetase. *J. Mol. Biol.* **2000**, *301*, 1257–1266.

(15) Kotnik, M.; Humljan, J.; Contreras-Martel, C.; Oblak, M.; Kristan, K.; Hervé, M.; Blanot, D.; Urleb, U.; Gobec, S.; Dessen, A.; Šolmajer, T. Structural and functional characterization of enantiomeric glutamic acid derivatives as potential transition state analogue inhibitors of MurD ligase. *J. Mol. Biol.* **2007**, *370*, 107–115.

(16) Humljan, J.; Kotnik, M.; Contreras-Martel, C.; Blanot, D.; Urleb, U.; Dessen, A.; Šolmajer, T.; Gobec, S. Novel naphthalene-*N*-sulfonyl-D-glutamic acid derivatives as inhibitors of MurD, a key peptidoglycan biosynthesis enzyme. *J. Med. Chem.* **2008**, *51*, 7486–7494.

(17) Tanner, M. E.; Vaganay, S.; van Heijenoort, J.; Blanot, D. Phosphinate Inhibitors of the D-glutamic acid-adding enzyme of peptidoglycan biosynthesis. *J. Org. Chem.* **1996**, *61*, 1756–1760.

(18) Štrancar, K.; Blanot, D.; Gobec, S. Design, synthesis and structure-activity relationships of new phosphinate inhibitors of MurD. *Bioorg. Med. Chem. Lett.* **2006**, *16*, 343–348.

(19) Perdih, A.; Kovač, A.; Wolber, G.; Blanot, D.; Gobec, S.; Šolmajer, T. Discovery of novel benzene 1,3-dicarboxylic acid inhibitors of bacterial MurD and MurE ligases by structure-based virtual screening approach. *Bioorg. Med. Chem. Lett.* **2009**, *19*, 2668–2673.

(20) Turk, S.; Kovač, A.; Boniface, A.; Bostock, J. M.; Chopra, I.; Blanot, D.; Gobec, S. Discovery of new inhibitors of the bacterial peptidoglycan biosynthesis enzymes MurD and MurF by structure-based virtual screening. *Bioorg. Med. Chem.* **2009**, *17*, 1884–1889.

(21) Horton, J. R.; Bostock, J. M.; Chopra, I.; Hesse, L.; Phillips, S. E.; Adams, D. J.; Johnson, A. P.; Fishwick, C. W. Macrocyclic inhibitors of the bacterial cell wall biosynthesis enzyme MurD. *Bioorg. Med. Chem. Lett.* **2003**, *13*, 1557–1560.

(22) Paradis-Bleau, C.; Beaumont, M.; Boudreault, L.; Lloyd, A.; Sanschagrin, F.; Bugg, T. D.; Levesque, R. C. Selection of peptide inhibitors against the *Pseudomonas aeruginosa* MurD cell wall enzyme. *Peptides* **2006**, *27*, 1693–1700.

(23) Kristan, K.; Kotnik, M.; Oblak, M.; Urleb, U. New high-throughput fluorimetric assay for discovering inhibitors of UDP-*N*-acetylmuramyl-L-alanine:D-glutamate (MurD) ligase. *J. Biomol. Screening* **2009**, *14*, 412–418.

(24) Kotnik, M.; Štefanič Anderluh, P.; Preželj, A. Development of novel inhibitors targeting intracellular steps of peptidoglycan biosynthesis. *Curr. Pharm. Des.* **2007**, *13*, 2283–2309.

(25) Šink, R.; Kovač, A.; Tomašić, T.; Rupnik, V.; Boniface, A.; Bostock, J.; Chopra, I.; Blanot, D.; Peterlin Mašič, L.; Gobec, S.; Zega, A. Synthesis and biological evaluation of *N*-acylhydrazones as inhibitors of MurC and MurD ligases. *ChemMedChem* **2008**, *3*, 1362–1370.

(26) Tomašić, T.; Zidar, N.; Kovač, A.; Turk, S.; Simčič, M.; Blanot, D.; Müller-Premru, M.; Filipič, M.; Grdadolnik, S. G.; Zega, A.; Anderluh, M.; Gobec, S.; Kikelj, D.; Peterlin Mašič, L. 5-Benzylidenethiazolidin-4-ones as Multitarget Inhibitors of Bacterial Mur Ligases. *ChemMedChem* **2010**, *5*, 286–295.

(27) Tomašić, T.; Zidar, N.; Rupnik, V.; Kovač, A.; Blanot, D.; Gobec, S.; Kikelj, D.; Peterlin Mašič, L. Synthesis and biological evaluation of new glutamic acid-based inhibitors of MurD ligase. *Bioorg. Med. Chem. Lett.* **2009**, *19*, 153–157.

(28) Zidar, N.; Tomašić, T.; Šink, R.; Rupnik, V.; Kovač, A.; Turk, S.; Patin, D.; Blanot, D.; Contreras Martel, C.; Dessen, A.; Müller Premru, M.; Zega, A.; Gobec, S.; Peterlin Mašič, L.; Kikelj, D. Discovery of novel 5-benzylidenerhodanine and 5-benzylidenethiazolidine-2,4-dione inhibitors of MurD ligase. *J. Med. Chem.* **2010**, *53*, 6584–6594.

(29) GOLD, version 4.1, is available from The Cambridge Crystallographic Data Centre, 12 Union Road, Cambridge, CB2 1EZ, U.K.; www.ccdc.cam.ac.uk.

(30) Baell, J. B.; Holloway, G. A. New substructure filters for removal of pan assay interference compounds (PAINS) from screening libraries and for their exclusion in bioassays. *J. Med. Chem.* **2010**, *53*, 2719–2740.

(31) Baell, J. B. Observations on screening-based research and some concerning trends in the literature. *Future Med. Chem.* **2010**, *2*, 1529–1546.

(32) Šink, R.; Gobec, S.; Pečar, S.; Zega, A. False positives in the early stages of drug discovery. *Curr. Med. Chem.* **2010**, *17*, 4231–4255.

(33) Jones, G.; Willett, P.; Glen, R. C.; Leach, A. R.; Taylor, R. Development and validation of a genetic algorithm for flexible docking. *J. Mol. Biol.* **1997**, *267*, 727–748.

(34) Nolte, R. T.; Wisely, G. B.; Westin, S.; Cobb, J. E.; Lambert, M. H.; Kurokawa, R.; Rosenfeld, M. G.; Willson, T. M.; Glass, C. K.; Milburn, M. V. Ligand binding and co-activator assembly of the peroxisome proliferator-activated receptor-gamma. *Nature* **1998**, *395*, 137–143.

(35) Benardeau, A.; Benz, J.; Binggeli, A.; Blum, D.; Boehringer, M.; Grether, U.; Hilpert, H.; Kuhn, B.; Marki, H. P.; Meyer, M.; Puntener, K.; Raab, S.; Ruf, A.; Schlatter, D.; Mohr, P. Aleglitazar, a new, potent, and balanced dual PPARalpha/gamma agonist for the treatment of type II diabetes. *Bioorg. Med. Chem. Lett.* **2009**, *19*, 2468–2473.

(36) Ishida, T.; In, Y.; Inoue, M.; Ueno, Y.; Tanaka, C.; Hamanaka, N. Structural elucidation of epalrestat(ono-2235), a potent aldose reductase inhibitor, and isomerization of its double-bonds. *Tetrahedron Lett.* **1989**, *30*, 959–962.

(37) Zidar, N.; Kladnik, J.; Kikelj, D. A convenient synthesis of 4-benzyl-2-(2-(4-oxo-2-thioxothiazolidin-5-ylidene)ethyl)-2*H*-1,4-benzoxazin-3(4*H*)-ones and 5-(2-(4-benzyl-3-oxo-3,4-dihydro-2*H*-1,4-benzoxazin-2-yl)ethylidene)thiazolidine-2,4-diones. *Acta Chim. Slov.* **2009**, *56*, 635–642.

(38) Boros, E. E.; Thompson, J. B.; Katamreddy, S. R.; Carpenter, A. J. Facile reductive amination of aldehydes with electron-deficient anilines by acyloxyborohydrides in TFA: application to a diazaindoline scale-up. *J. Org. Chem.* **2009**, *74*, 3587–3590.

(39) Percec, V.; Imam, M. R.; Peterca, M.; Wilson, D. A.; Heiney, P. A. Self-assembly of dendritic crowns into chiral supramolecular spheres. *J. Am. Chem. Soc.* **2009**, *131*, 1294–1304.

(40) Lanzetta, P. A.; Alvarez, L. J.; Reinach, P. S.; Candia, O. A. Improved assay for nanomole amounts of inorganic-phosphate. *Anal. Biochem.* **1979**, *100*, 95–97.

(41) McGovern, S. L.; Helfand, B. T.; Feng, B.; Shoichet, B. K. A specific mechanism of nonspecific inhibition. *J. Med. Chem.* **2003**, *46*, 4265–4272.

(42) Brooks, B. R.; Bruccoleri, R. E.; Olafson, B. D.; States, D. J.; Swaminathan, S.; Karplus, M. Charmm: a program for macromolecular energy, minimization, and dynamics calculations. *J. Comput. Chem.* **1983**, *4*, 187–217.

(43) Halgren, T. A. Merck molecular force field. 1. Basis, form, scope, parameterization, and performance of MMFF94. *J. Comput. Chem.* **1996**, *17*, 490–519.

(44) Accelrys Discovery Studio is available from Accelrys Inc., San Diego, CA 92121, U.S.

(45) Pymol is available from Delano Scientific LLC, San Francisco, CA; http://pymol.sourceforge.net.